The effect of different surface topographies on the corrosion behaviour of nickel

A. S. Toloei, V. Stoilov & D. O. Northwood
Department of Mechanical, Automotive and Materials Engineering, University of Windsor, Ontario, Canada

Abstract

The electrochemical and corrosion behaviour of a surface is extremely complicated and depends on various chemical, physical and mechanical factors. In this study the effect of different surface roughnesses on the corrosion resistance of nickel in 0.5 M sulphuric acid was investigated. Open circuit potential, corrosion current density, polarization resistance and corrosion rate were measured for surfaces polished with different grits (120, 240, 400, 600 and 1200) of silicon carbide papers. The surface roughness was measured using a profilometry method both before and after corrosion testing. SEM images were taken and compared for all of the samples before and after corrosion tests. The results showed that surface roughness and surface morphology can considerably change corrosion and corrosion rate. A higher corrosion resistance is obtained for surfaces with lower roughnesses. Finally, the results were compared with specimens where a specific surface patterning was obtained using a laser ablation method.
Keywords: corrosion, nickel, surface roughness.

1 Introduction

There are many different methods of surface modification such as coatings, inhibitors and surface patterning to combat corrosion. Schweinsberg and Flitt [1] have shown that the purity of the anode and the electrolyte, the metallurgical history of the material and pre-treatment of the working electrode (abrasion technique, pre-polarization, time of immersion in the electrolyte) are amongst the most important parameters governing corrosion current density, and the corrosion rate. In different studies [2, 3], grain size, materials composition, mode

WIT Transactions on Engineering Sciences, Vol 77, © 2013 WIT Press
www.witpress.com, ISSN 1743-3533 (on-line)
doi:10.2495/MC130171

of manufacturing, geometry and roughness have been reported to be the most important parameters affecting corrosion potential and current density.

Among the investigated parameters, surface roughness has a major impact both on general corrosion, and the nucleation of metastable pitting and pitting potential [4]. Surface roughness is also known to affect the hydrodynamic and mass-transfer boundary layer, thus influencing the corrosion mechanism and rate [5]. Due to the significant effect of surface roughness on the corrosion resistance, it is possible to meet certain corrosion resistance requirements by specifying a surface finish rather than by upgrading the chosen alloy [6]. It has been shown that an increase in the surface roughness of stainless steels increases the pitting susceptibility and general corrosion rate which is attributed to the passive film breakdown. Behaviour similar to stainless steel has also been observed in copper, aluminium and titanium-based alloys [7–9]. In the case of mild steels, however, a reverse trend has been reported [6]. Also, Alvarez et al. in their work on AE44 magnesium alloy have shown corrosion behaviour consistent with mild steels and opposite to the trend reported in stainless steels [10]. Despite the significant attention that has been paid to the influence of the surface roughness on the pitting corrosion resistance in stainless steels, very little is known of the influence of the surface roughness on the general corrosion resistance [11]. In addition, to the author's best knowledge, there have been no studies on the effect of surface roughness on the corrosion behaviour of nickel and its alloys.

In this study, the corrosion of nickel in dilute sulphuric acid was studied through a potentiodynamic polarization technique to calculate open circuit potential, E_{corr} R_P and I_{corr} values for different surface roughnesses. SEM images were taken and compared for all of the samples and profilometry test measured the roughness of samples before and after corrosion tests. The results were compared with those for samples prepared with specific surface patterning.

2 Experimental procedures

2.1 Sample preparation

Nickel was used as a sample material for this study. All the specimens were cut to 15 × 15 × 1 mm size. Two types of surface modification have been applied, surface roughness obtained through grinding and predesigned surface patterns. The roughness was varied by polishing with SiC papers of different grades, including grit numbers 120, 240, 400, 600 and 1200. A smaller grit number represents a rougher finish. It should be mentioned that the grinding process was performed in one direction only. The 1200 grit surface was further polished with 0.05 μm alumina paste. The letter G, in the used notation, stands for grit, whereas samples with predesigned surface patterns were labelled using DxLy format where D is the hole diameter and L is the inter-hole spacing. The predesigned surface patterns were created using laser ablation. The surface patterns were based on the repetition of holes in the form of equilateral triangles in both X and Y directions. To create the holes, a copper bromide laser was used and single pulse was applied. Nitrogen gas was blown in order to protect the

surface from oxidation. To assure repeatability, five sets of specimens were prepared and tested and all reported results are mean values.

2.2 Corrosion testing

Before each electrochemical experiment the specimens were degreased with ethanol and rinsed with deionized water and then immersed in a cell containing the electrolyte. This was followed by leaving the working electrode (WE) at open-circuit potential (OCP) for 30 min before the subsequent corrosion measurements. Corrosion tests were carried out in a 0.5 M H_2SO_4 solution at 23±1°C using a CHI660D, Electrochemical Workstation Beta, (version 11.17). A standard three-electrode cell was used. The counter electrode (CE) was a high-purity Pt electrode, while the reference electrode (RE) was a saturated calomel reference electrode (SCE). The working electrode (WE) was a nickel sample of surface area of 1 cm^2 exposed to the electrolyte. Polarization resistance (R_p), I_{corr} and corrosion rate values of the nickel samples were calculated using the linear polarization method as obtained from eqn (1):

$$R_p = \beta_a\beta_c/2.3i_{corr}(\beta_a + \beta_c) \quad (1)$$

where β_a and β_c are cathodic and anodic Tafel constants and i_{corr} is the corrosion current density obtained from a potentiodynamic curve [12].

2.3 Surface morphology

A Wyko Surface Profiling System NT-1100 was used to measure surface roughness parameters and obtain 3-dimensional topographical map of the tested surfaces. In order to describe the unique features of the surfaces, roughness parameters such as, the average surface roughness (R_a) and the root mean square average roughness (R_q) have been used [13]. In this study we report R_a values.

Scanning electron microscopy (SEM) and energy-dispersive x-ray spectrometry (EDS) were used to compare the surface structure and composition before and after potentiodynamic testing.

3 Results

3.1 Corrosion testing

Table 1 shows the mean calculated values for corrosion parameters of samples with different surface roughness. As can be seen both from Table 1and in Figure 1, which shows the potentiodynamic polarization curves for samples prepared using different grit sizes, the corrosion potential (E_{corr}) shifted towards the noble direction as the surface roughness decreased. Table 1 also shows that the corrosion current (i_{corr}) decreased as the surface roughness decreased. However, no significant difference was observed in cathodic currents among the samples with different surface roughness: (see Figure 1). This suggested that the shift in the E_{corr} and the variation in i_{corr} were primarily due to the anodic behaviour of the alloy. The specimens with the highest surface roughness

showed a sharper increase in the anodic current just above the E_{corr}. This phenomenon can be an indication of pitting [10]. If the pitting potential of all samples is considered at a specific current value (Figure 1), it becomes obvious that in the sample with lowest roughness (G1200) the onset of pitting is shifted to higher potential [9]. In each of the curves in Figure 1, there is a point immediately after the passive region, where the current density begins to rise (Points a, b and c). The breakdown of the protective film begins at that point which is known as critical pitting or breakdown potential. This is where the likelihood of pitting is the greatest and the point is used as a parameter for assessing pitting properties of the tested materials. This point happens at higher potential values for surfaces with lower roughness values.

Table 1: Corrosion parameters calculated for different surface roughnesses.

Sample	E_{corr} (mV)	i_{corr} ($\mu A/cm^2$)	β_a (mV)	β_c (mV)	R_P (Ω/cm^2)
G120	-321.8	21.64	109.5	118.3	1.14×10^3
G240	-310.5	19.27	110.0	116.8	1.27×10^3
G400	-313.9	17.26	112.1	113.3	1.41×10^3
G600	-312.6	14.67	123.8	111.1	1.73×10^3
G1200	-272.7	8.43	120.3	105.3	2.9×10^3
D10L20	-327.4	6.01	153.4	128.5	5.04×10^3
D20L20	-303.3	1.16	132.6	173.3	28.07×10^3

Figure 2 illustrates the variation in the corrosion rate with respect to surface roughness (R_a). Clearly, the corrosion rate decreases with decrease in roughness. In addition, it has been observed an increase of the number of pits on the rougher surfaces compared to the smooth surface [14]. This implies that the formation of metastable pits on a smooth surface is more difficult than that on a rougher surface, which corresponds to a lower corrosion rate. The result is consistent with similar studies which show that a higher roughness corresponds to a lower pitting potential (the potential at which metastable pits start to form on the surface) [14].

The patterned samples created by laser ablation, showed significantly lower corrosion rates than the samples with random roughness (Red points in figure 2). The main mechanism behind the significant decrease in the corrosion rate has been shown to be heterogeneous wetting [15, 16]. Heterogeneous wetting results in formation of alternating solid/liquid zones and stable air/vapour pockets. The air/vapour pockets allow the formation of the passive oxide layer but prevent its dissolution by the electrolyte. The heterogeneous interface, formed between the solution and the surface, significantly decreases the overall contact area between the surface and the electrolyte, thus significantly decreasing the corrosion rate [15, 16].

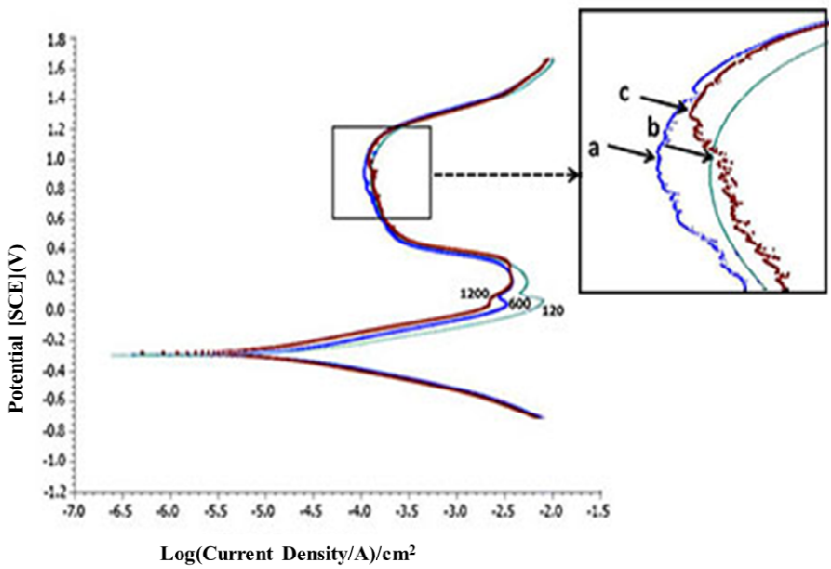

Figure 1: Potentiodynamic polarization curves for ground samples (120, 600 and 1200 grit).

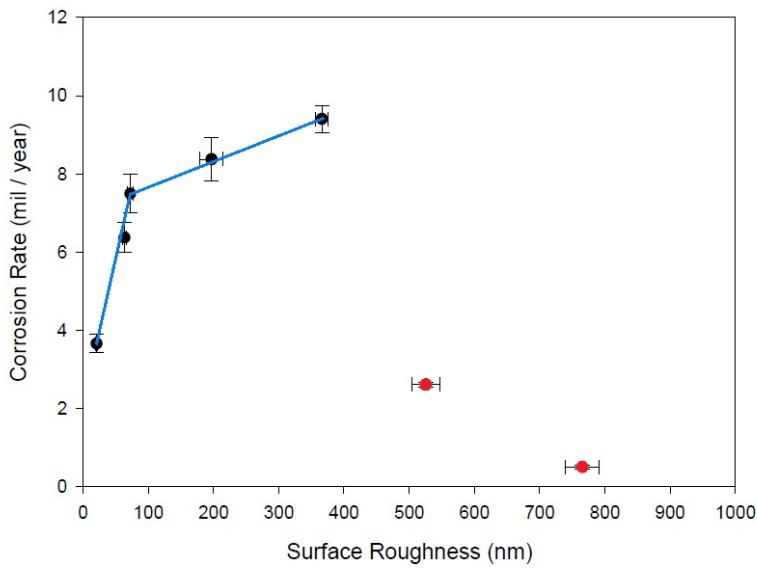

Figure 2: Corrosion rate values for different surface roughnesses.

3.2 Surface roughness measurement

The average roughness value for samples G120 to G1200 and two patterned samples before and after corrosion testing are presented in Figure 3. As it can be seen, for samples G120 through G1200, as grit number increased, the roughness value decreased before corrosion testing. The same trend is almost seen after corrosion testing but with higher roughness values for all samples. In contrast, the samples with predesigned surface patterns, D10L20 and D20L20, had higher roughness values but significantly lower roughness change after corrosion testing compared to the samples with the unidirectional grinding roughness.

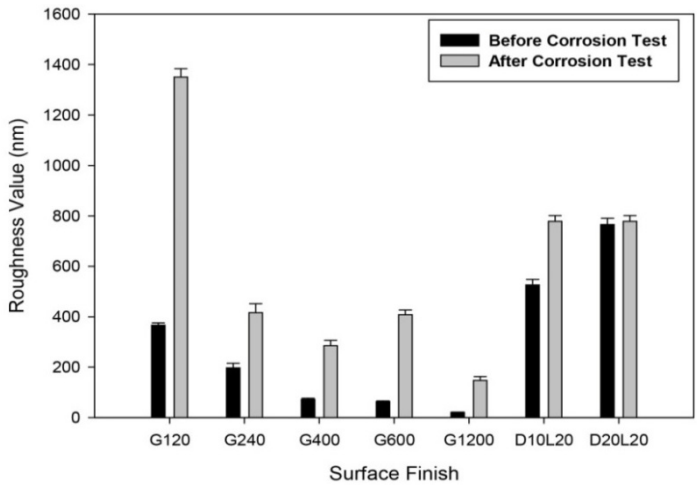

Figure 3: Roughness values before and after corrosion test.

All samples, however, show higher roughness values after corrosion testing. Figures 4(a) and (b) show the 3D topography images for samples G240 before and after corrosion tests. It is obvious that the uniform area has changed to a surface with deeper grooves with higher roughness which is a result of the corrosion process. Diffusion of corrosion products in deeper grooves is limited, hence the solution condition for local dissolution of metal is easily satisfied [4]. This means that on rougher surfaces more metastable pits are formed and the active sites on these surfaces have lower openness (ratio of width to depth at opening of the grooves), hence have a higher possibility to grow larger. Higher depth to width values are reported to indicate more smooth surfaces and it is more difficult to form micro-pits [4].

3D roughness images for the patterned samples showed brighter colour of the surface after corrosion (dark colours show deep point like grooves) which showed surface roughness has increased and no severe corrosion was observed. In these 3D images there was no significant change in the surface appearance (which is in agreement with the SEM images: see section 3.3). It seems that both surfaces, before and after corrosion tests, are almost identical, which reaffirms the results from the potentiodynamic corrosion rate tests.

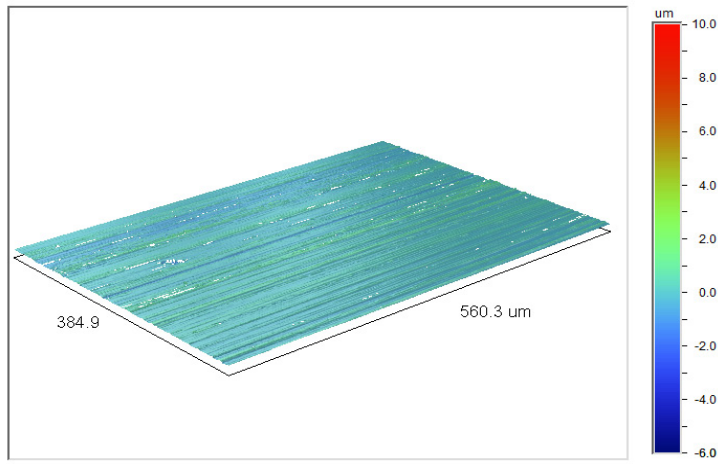

(a)

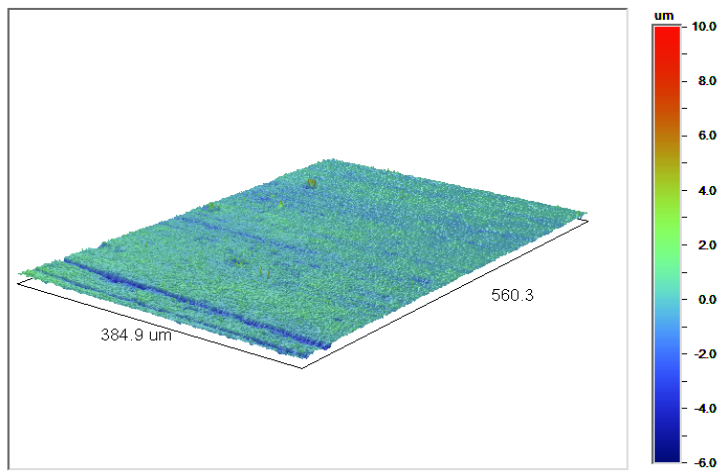

(b)

Figure 4: Sample G240 3D roughness (a) before and (b) after corrosion testing.

3.3 Scanning electron microscopy

Figures 5(a)–(d) are SEM images of samples G120 and G240 before and after corrosion. For G120, (Figures 5 (a), (b)), the corrosion is concentrated along the grooves. By decreasing the roughness from sample G120 to G240, (Figures 5 (c), (d)) less surface degradation is observed after corrosion testing. By comparing

this sample before and after the corrosion test it can be observed that the sample has been corroded and the grooves' contrast (depth) is not as visible as before the test. This leads to the conclusion that in this sample the corrosive solution has reached the whole surface including the bottom of the grooves. Corrosion for rougher sample (G120) is more severe compared to the smoother one (G240). The micrograph also shows that the corrosion pits were preferentially aligned along the grooves suggesting that the deep valleys on the ground surface were favourable sites for pit nucleation [13]. The result is in agreement with the measured corrosion potential, corrosion rate and roughness observations. In all cases by increasing the roughness a higher corrosion rate has been recorded.

The surface microstructure for the patterned samples before and after corrosion tests was also analysed and the corresponding SEM micrographs were obtained. Figures 5(e) and (f) illustrate the patterned sample before and after the corrosion tests. In the SEM images there is not a significant change in the surface appearance (good agreement with the 3D profilometry images). This is also in agreement with the measured corrosion rate values. In this case, no severe corrosion has occurred, mainly due to the existence of heterogeneous wetting [15].

3.4 Energy-dispersive x-ray spectrometry (EDS)

The main goal of the EDS examination was to evaluate the change in O concentration on the surface of the samples. In the spectrum, three elements, nickel (Ni), oxygen (O) and carbon (C) were observed. The intensity of the largest peaks (Ni: Lα=0.851 and O: Kα=0.523 KeV) was used to calculate the oxygen concentration on the surface (see Table 2).

Table 2: Oxygen content before and after corrosion testing.

Oxygen %wt	Before corrosion	After corrosion
G120	1.37	4.71
G240	1.20	3.6
G400	1.20	2.11
G600	1.48	3.69
G1200	1.49	3.75

All samples had similar oxygen contents before corrosion testing and this value increased for all samples after corrosion testing. In samples with higher corrosion rates, the reason for increased oxygen concentration is the autocatalytic diffusion and corrosion process happened within the grooves which resulted in degradation of metal [6, 7, 9, 13]. In the case of samples with lower corrosion rate the increase of oxygen content was a result of a stable passive layer which was formed on the surface [9].

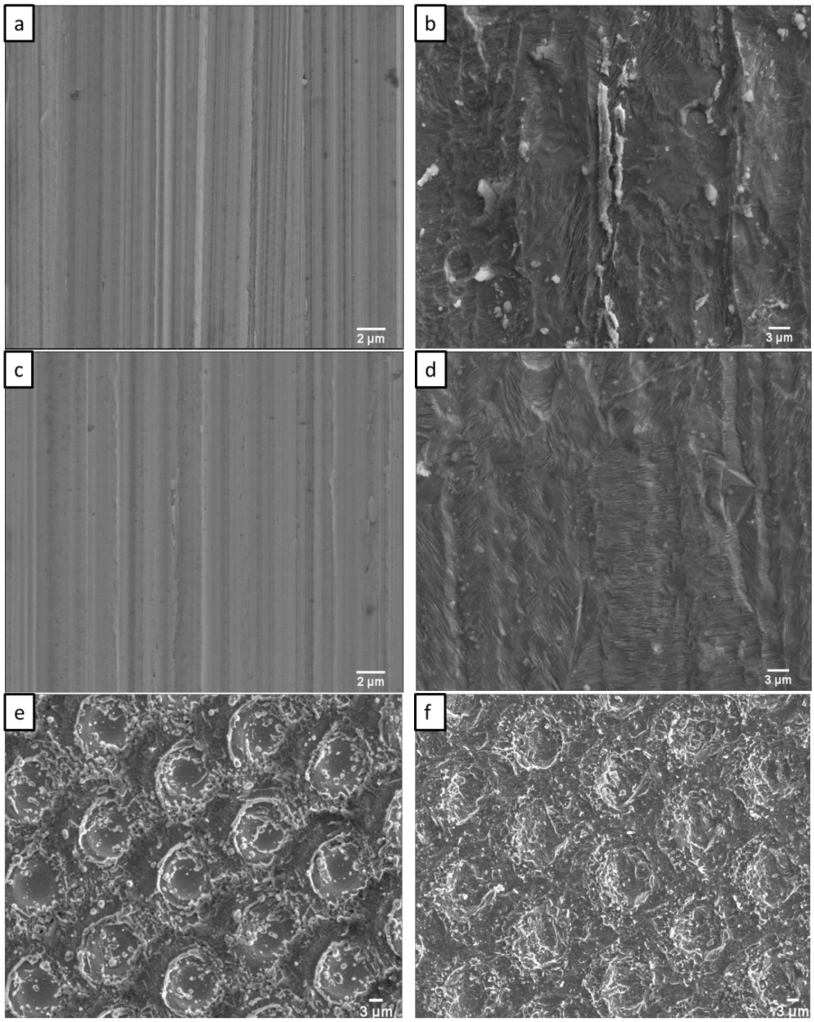

Figure 5: SEM of the sample G120 (a) before and (b) after corrosion, sample G240 (c) before and (d) after corrosion and sample D10L20 (e) before and (f) after corrosion.

4 Discussion

Based on the measured corrosion potentials and corrosion rates, it can be concluded that the corrosion rate of nickel increased with an increase of surface roughness. The reason for this phenomenon is that by increasing the roughness the active sites increased and deeper grooves played an active role as suitable places for localized corrosion. The depth of the valleys that influenced the

diffusion of active ions during corrosion and IR drops in the deep valleys seem to be important parameters that affect the corrosion rate. On the rougher surfaces, the grooves trap the corrosion products, which results in more pitting [13]. In a smooth surface the frequency of metastable pitting is reduced because of the number of available metastable pit sites is reduced and consequently the corrosion rate is decreased [17]. Also, in a smooth surfaces weak points are less " activate " than on rough surfaces and the formation of stable passive film on smooth surfaces is more likely to occur. All the EDS results of nickel samples in this study showed an increase in oxygen content. For surfaces with low roughness values this increase in oxygen content can be related to the oxide layer formation. The presence of a protective oxide film lowers the activity of substrate/bulk interface. On rougher surfaces, compared to smooth surfaces, diffusion processes at nucleation sites in small scratches are hindered and there is a higher probability of accumulation of aggressive species and the geometry of small scratches make it easier to maintain a high potential drop [9]. But when the surface is smooth, the pit will survive more due to the formation of lace cover on the pit mouth maintaining the diffusion process which will result in less corrosion on the surface [6].

Rougher surfaces of a metal exhibit lower pitting potentials because by increasing the roughness less-open pit sites are maintained during the early stages of growth as metastable pits. Therefore, there is more restricted diffusion of metal cations during propagation which will result in the transition from metastable to stable pit growth to be made at lower potentials and consequently lower the pitting potential. It is said that deeper, less-open pit site has a greater probability of generating a pit, than a shallower, more-open one. Since the sites on the rougher surfaces are more occluded than those of smoother surfaces, it follows that pits growing on the rougher surface have a greater chance of survival to the stable growth stage, and thereby show a lower pitting potential [7, 8]. On a passive metal, rougher surfaces are more susceptible than smoother surfaces to localised forms of corrosion such as pitting and crevice corrosion. This effect can be related to the surface nucleation of metastable pitting preceding propagation of pitting. Although a higher number of nucleation events take place on a smoother surface as compared to a rough surface [8], propagation of the pits and formation of micropits does not occur as readily [4, 8]. On a rougher surface, several of these nucleation events will lead to propagation of pits and thereby corrosion [3].

In patterned samples, the formation of the passive oxide layer inside the pattern holes prevents the electrolyte reaching the bottom of the patterned hole. In other words, the contact between the electrolyte and the metal surface is heterogeneous wetting–alternating solid/liquid zones and stable air/vapour pockets. The air/vapour pockets allow the formation of the passive oxide layer but prevent its dissolution by the fluid. The heterogeneous interface, formed between the solution and the surface, decreases the overall contact area between the surface and the electrolyte, thus significantly decreasing the corrosion rate [15].

5 Conclusions

This study demonstrates that surface morphology makes a significant contribution to corrosion. For materials and environments where a passive film formed, as surface roughness decreased, both the corrosion potential and the pitting potential shifted to more noble values. The observed trends include: the rough surfaces limit diffusion out of the formed grooves; more available active sites on the rough surfaces; and there is fast formation of a stable oxide film on the smoother surfaces. When the material has the ability to form a passive film quickly, as is the case with nickel, aluminium and stainless steel, the rougher surface would be easily pitted because the smooth surface has fewer places for pit nucleation and can quickly form a passive film preventing pit nucleation. SEM and EDS results supported the conclusion of more corrosion on rougher surfaces and the formation of oxide layer on the surface. Specific surface patterning can further reduce the corrosion rate through a process of heterogeneous wetting.

References

[1] Schweinsberg, D. and Flitt, H.J., Some practical considerations relevant to the recording of corrosion data. *Corrosion & Prevention,* **45**, pp. 541-553, 2005.

[2] Alvarez, R., Martin, H., Horstemeyer, M. and Chand, M., Corrosion relationships as a function of time and surface roughness on a structural AE44 magnesium alloy. *Corrosion Science,* **52**, pp. 1635-1648, 2010.

[3] Hilberta, L., Bagge-Ravnb, D., Koldc, J. and Gram, L., Influence of surface roughness of stainless steel on microbial adhesion and corrosion resistance. *International Biodeterioration & Biodegradation,* **52**, pp. 175-185, 2003.

[4] Zuo, Y., Wang, H. and Xiong, J., The aspect ratio of surface grooves and metastable pitting of stainless steel. *Corrosion Science,* **44**, pp. 25-35, 2002.

[5] Asma, R.N., Yuli, P. and Mokhtar, C., Study on the effect of surface finish on corrosion of carbon steel in CO2 environment. *Journal of Applied Sciences,* **11**(**11)**, pp. 2053-2057, 2011.

[6] Abosrra, L. Ashour, A., Mitchell, S.C. and Youseffi, M., Corrosion of mild steel and 316L austenitic stainless steel with different surface roughness in sodium chloride saline solutions. *WIT Transactions on Engineering Sciences,* **65**, pp. 161-172, 2009.

[7] Sasaki, K. and Burstein, G., The generation of surface roughness during slurry erosion-corrosion and its effect on the pitting potential. *Corrosion Science,* **38**(**12)**, pp. 2111-2120, 1996.

[8] Burstein, G. and Vines, S., Repetitive nucleation of corrosion pits on stainless steel and the effects of surface roughness. *Journal of The Electrochemical Society,* **148**(**12)**, pp. B504-B516, 2001.

[9] Suter, T., Muller, Y., Schmutz, P. and Van Trzebi, O., Microelectrochemical studies of pit initiation on high purity and ultra high

purity aluminium. *Advanced Engineering Materials,* **7(5)**, pp. 339-348, 2005.
[10] Walter, R. and Bobby Kannan, M., Influence of surface roughness on the corrosion behaviour of magnesium alloy. *Materials and Design,* **32**, pp. 2350-2354, 2011.
[11] Shahryari, A., Kamal, W. and Omanovic, S., The effect of surface roughness on the efficiency of the cyclic potentiodynamic passivation (CPP) method in the improvement of general and pitting corrosion resistance of 316LVM stainless steel. *Materials Letters,* **62**, pp. 3906-3909, 2008.
[12] Roberge, P., *Corrosion Engineering Principles and Practice*, McGraw-Hill, New York, 2008.
[13] Mok Lee, S., Gyu Lee, W., Ho Kim, Y. and Jang, H., Surface roughness and the corrosion resistance of 21Cr ferritic stainless steel. *Corrosion Science,* **63**, pp. 404-409, 2012.
[14] Li, W. and Li, D., Influence of surface morphology on corrosion and electronic behaviour. *Acta Materialia,***54**, pp. 445-452, 2006.
[15] Toloei, A., Stoilov, V. and Northwood, D., The effect of creating different size surface patterns on corrosion properties of Nickel. *ASME International Mechanical Engineering Congress & Exposition, IMECE2012*, Houston, 2012.
[16] Bigdeli Karimi, M. Stoilov, V. and Northwood, D., Improving corrosion performance by surface patterning. WIT Transactions on Engineering Sciences, **72**, pp. 85-93, 2011.
[17] Burstein, G. and Pistorius, P., Surface roughness and the metastable pitting of stainless steel in chloride solutions. *Corrosion,* **51(5)**, pp. 380-385, 1995.